

Scale Model Testing of a Submersible Aquaculture Cage

Zachary Davonski, Kathryn Trubac

Advisors: M. Robinson Swift, Corey Sullivan

ABSTRACT

Net pen aquaculture provides a viable solution to the food crisis associated with the rapid expansion of the global population. A scale physical model of the StormSafe Submersible Net Pen, a system proven successful in the Great Lakes, was tested in the UNH wave tank. The submersible capability of the cage relies on variable water ballast that enables rapid submergence to avoid damage from storms and ice flows. Its success and versatility have prompted interest in its use in marine environments, hence this project investigates the suitability of StormSafe for an open ocean location, via the construction and testing of a 1/15th Froude-scale model. The model is scaled based on the depths of the UNH wave tank and a potential ocean deployment site, 8 miles south of Long Island, NY. Testing involved subjecting the model to simulated ocean waves and currents in order to analyze the response of both the cage and mooring system. Wave testing was performed for surfaced and submerged configurations with wave heights corresponding to ocean conditions. The current testing simulated the maximum tidal currents observed at the Long Island site. Based on preliminary results, StormSafe shows promise for use in open-ocean aquaculture.

I. INTRODUCTION

A. Purpose

In this project the StormSafe Submersible Net Pen was investigated for use in open ocean environments. The original design was Froude-scaled, and a 1/15th scale model was fabricated for testing in the UNH wave tank. Simulated current testing was done to determine the drag force on the cage in both the surface and submerged configurations. Wave testing was also conducted on the cage to determine the loading in the mooring system and the motion response of the cage when exposed to waves. Based on the results from conducting these tests, it will be determined whether or not the StormSafe Submersible design is suitable for open ocean environments.

B. Background

Mike Meeker has been raising fish for over 30 years on Manitoulin Island in Lake Huron. Throughout his decades of experience, he has learned both what is successful, and what is problematic in the growout of freshwater finfish. After multiple iterations of cage designs, and two winters that completely decimated his farm due to ice flows, he created StormSafe. StormSafe is a fully submersible, modular, and simplistic net pen with high capacity and minimal infrastructure. The submersible capability of the cage relies on variable water ballast that enables rapid submergence to avoid damage from storms and ice flows. Meeker Aquaculture

has been successfully using the StormSafe Submersible Net Pen to grow rainbow trout for several years now.

StormSafe was designed to address two major causes of damage in the Great Lakes environment: ice flows and storm conditions. However, these problems are not unique to the Great Lakes. Every net pen farmer throughout the world has to contend with similar issues, even those operating in a marine environment. Therefore, there is serious interest in the use of StormSafe for offshore net pen aquaculture. Manna Fish Farms, a New York based company, has a vested interest in deploying these cages in the North Atlantic Ocean. Manna's intended farm site is 8 miles off the south shore of Long Island, in depths of approximately 120 ft and maximum current speeds of roughly 0.6 m/s.

C. Objectives

- Fabricate scale model to analyze response to ocean conditions
- Test model in UNH wave tank
- Analyze results to determine the adequacy of design for an ocean environment

D. Approach

In order to construct a scale model of the StormSafe Submersible Net Pen, the components needed to be scaled down from the original design. Once each component was sized correctly, the appropriate materials needed to be determined and sourced. Fabrication of the model began when all the components were as close as possible to Froude-scale specifications. As soon as the model was constructed, hydrostatic testing was done to evaluate its stability and non-ballasted buoyancy. Full scale centers of gravity for the two configurations were calculated, making it possible to determine the amount of ballast needed to achieve the desired model depths, which were approximately 2 inches above the surface of the water and 1 ft below. Once the drafts were determined, the model could undergo current testing in order to determine the force of drag on the cage. The next step was to prepare the setup for wave testing. To do this, the mooring system was fabricated and installed in the tank. This would allow for the cage to be subjected to waves, which would determine the wave induced mooring loads and its motion response. Analysis of the data will determine if the cage design is suitable for open ocean environments.

II. STORMSAFE SITE VISIT

A trip to the Meeker Aquaculture facilities was taken in the early stages of the project in order to gain a better understanding of the StormSafe Submersible Net Pen. Discussions with Mike Meeker, coupled with seeing the cage firsthand provided details on the dynamics of the cage and the specifics of its components. Specifically, flooding combinations for the submergence of the cage were investigated. This provided a better understanding of the submergence procedure for the cage, so that the model would be as accurate to the full-scale cage as possible. In addition to determining the dynamics of the cage during the site visit, specific dimensions were confirmed. This included the diameters of the rope used for the mooring lines, and the exact setup of the mooring system. It was determined that the mooring lines between the buoys and the anchors

were almost completely vertical, and the bridle line from the buoy was attached to the top of the spars of the cage. This solidified the design for the scaled version of the mooring system used in wave testing.

III. PHYSICAL MODEL DESIGN

A. Froude Scaling

The properties of the scale model as well as the parameters of the testing to be performed were all determined via Froude scaling. Froude scaling maintains geometric, kinematic, and dynamic similitude between a full-scale object and its model scale, determined by Froude number. Froude number (F_n) is the ratio of inertial forces to gravitational forces acting on an object. Matching F_n between the full and model scale ensures that all gravitational forces scale correctly between the two.

The scale ratio used in this project was based on the depths of the test environment (the UNH Wave Tank) and the intended ocean site. The average depth recorded at the Long Island site is approximately 120 ft, and the UNH Wave Tank has a uniform depth of 8 ft. The ratio of these depths determined the 1:15 scale the cage was built upon.

Scale ratios for Froude models

Parameter	Dimension	Froude	Reynolds
Geometric similarity			
Length	[L]	λ	λ
Area	[L ²]	λ^2	λ^2
Volume	[L ³]	λ^3	λ^3
Rotation	[-]	1	1
Kinematic similarity			
Time	[T]	$\lambda^{1/2}$	λ^2
Velocity	[LT ⁻¹]	$\lambda^{1/2}$	λ^{-1}
Acceleration	[LT ⁻²]	1	λ^{-3}
Discharge	[L ³ T ⁻¹]	$\lambda^{5/2}$	λ
Dynamic similarity			
Mass	[M]	λ^3	λ^3
Force	[MLT ⁻²]	λ^3	1
Pressure and stress	[ML ⁻¹ T ⁻²]	λ	λ^{-2}
Energy and work	[ML ² T ⁻²]	λ^4	λ
Power	[ML ² T ⁻³]	$\lambda^{7/2}$	λ^{-1}

Figure 1: How Froude scaling affects different parameters.

B. Materials

Due to financial, time, and logistics constraints, the materials used for the model were not the same materials used in the full scale. Therefore, model materials had to be carefully selected in order to ensure that certain characteristics were matched as best as possible. Weight distribution, submerged volume, and cross-sectional area were the three main parameters that material selection was based upon. Satisfying these conditions meant finding materials with the proper dimensions, densities, strengths, etc. Doing so proved non-trivial, as we were limited by product availability and expense. Each material was selected to the best of our ability within the constraints of the project.

C. Spars

1 ½ inch foam core ABS pipe was chosen for the six main spars of the model. With a density of .0313 lbs/in³, the resulting difference in mass between the model scale and actual was only 2%.

Component	Length [ft]			Diameter [in]			Mass [lbs]		
	FS	MS	Actual	FS	MS	Actual	FS	MS	Actual
Main Spar	49.5	3.3	3.3	30	2	1.95	3452	1.02	1.04

Table 1: Lengths, diameters, and masses of the spars between the full-scale, model scale, and actual model.

D. Pipe Walkways

1 ¼ inch PVC pipe was chosen for the six horizontal pipe walkways of the model. The full-scale component has decking that lies on top of it for maintenance and harvesting purposes. Due to its negligible area, the decking was omitted from the scale model, but its mass was accounted for in the weight of the pipe walkway. The pipe itself has a total of 42 holes cut out of the sides of the pipe to decrease fluid drag. Matching the amount of mass removed by these holes in the model proved difficult, as did selecting a material that properly accounted for the deck weight. Therefore, the actual mass of the pipe walkway component is greater than the model scale.

Component	Length [ft]			Diameter [in]			Mass [lbs]		
	FS	MS	Actual	FS	MS	Actual	FS	MS	Actual
Pipe Walkway	46.5	3.1	3.1	24	1.6	1.66	2787	.826	.948

Table 2: Lengths, diameters, and masses of the pipe walkways between the full-scale, model scale, and actual model.

E. Bottom Connectors

½ inch PVC pipe was chosen for the six horizontal bottom connectors of the model. This component is completely sealed off in the full scale and provides additional buoyancy for the cage. Therefore, the model scale bottom connectors needed to be water-tight as well.

Component	Length [ft]			Diameter [in]			Mass [lbs]		
	FS	MS	Actual	FS	MS	Actual	FS	MS	Actual
Bottom Connector	44.8	2.98	2.98	10.75	.717	.84	1301	.385	.4364

Table 3: Lengths, diameters, and masses of the bottom connectors between the full-scale, model scale, and actual model.

F. Hinges

Matching the strength and directions of motion of the full-scale joints and hinges was a priority of the design process. The joints between the spars and the pipe walkways are uni-directional, only allowing vertical motion between the two components. However, the joints between the spar and the bottom connectors are multi-directional, allowing for both vertical and horizontal motion of the two components. The model scale joints for the bottom of the spars were simulated via two steel screw eyes.

G. Mooring Line

The mooring lines used in the full-scale system are 1 ½ inch polysteel rope that has a maximum tensile strength of roughly 48,000 lbs. The same type and size of line was also used for cross-bracing between the top and bottom of each adjacent spar. The scaled down diameter of this line

had to be 0.1 inches or 2.54 mm. The original candidate for this line was 600 lb monofilament fishing leader with a diameter of 2.5 mm. It was used for the cross-bracing, however it proved to be too stiff and have too much memory to serve as the bridle/anchor lines of the mooring. Instead, 2.5 mm diameter synthetic nylon rope was used for the model scale mooring lines.

H. Buoys

The StormSafe mooring system utilizes six Polyform Aqua 850 surface buoys with a net buoyancy of 800 kg or 7848 N to support the weight of the cage when submerged. Finding an object with the same net buoyancy was unrealistic, so we created our own out of closed cell foam insulation board.

I. Shackles

All shackles and clevises of the full-scale mooring system were substituted with 75 lb fishing snap swivels.

IV. FABRICATION

A. Cage

i. Spars

Once the ABS pipes were trimmed to size on the band saw, a partially threaded PVC coupling was modified and affixed to the top and bottom of the spars to represent the full-scale top and bottom spar caps, as seen in Figure 2. 1 ½ inch gripper plugs were used in the top to allow for a removable water-tight seal. The bottoms of the spars were permanently sealed by using PVC cement to attach a 1/8 inch thick acrylic disk to the end.



Figure 2: Comparison between the top and bottom caps and joints of the full-scale and the actual model.

ii. Pipe Walkway

The holes in the pipe walkways were drilled using a hole-saw bit in the drill press. Since the mass of the pipe walkway components was too high, channels in the tops and bottoms of the pipe were drilled to reduce the mass of these components, seen in Figure 3. These channels were drilled out with the drill press and then finished with a Dremel tool. While this reduced the weight, the actual mass of the pipe walkway components was still larger than what they should be in the model.

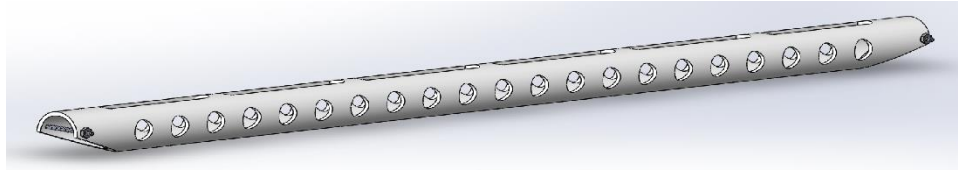


Figure 3: SolidWorks simulated pipe walkway component of the scale model.

iii. Bottom Connectors

For construction of the bottom connectors, once again 1/8 inch thick acrylic disks were PVC cemented to the ends of the pipe. Then 1/2 inch PVC caps were placed on the ends of the pipes to represent the full-scale bottom connector end caps, as well as to serve as a surface to attach the screw eyes to. These fittings were done this way to prevent water from entering the bottom connectors. This allowed for the bottom connectors to be completely full of air, with no adjustable ballast. This component can be seen in Figure 4.

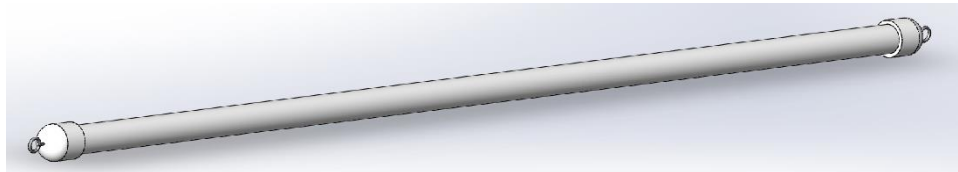


Figure 4: SolidWorks simulated bottom connector component of the scale model.

iv. Hinges

The steel screw eyes used were embedded in the bottom cap of the spar and in the end cap of the bottom connector. The eye loop of both screw eyes was trimmed and then they were attached at 90 degrees to each other and the loops were closed. Completely closing the loops restricted motion in directions other than the vertical and horizontal to the greatest possible extent. The joints at the top of the spar had one trimmed screw eye in the top cap of the spar, with a horizontal bolt at the end of the pipe walkway that slid through the screw eye, seen in Figure 5. The bolt acts as a hinge pin, and allows the components to move strictly up and down.



Figure 5: Scale model screw eyes used to simulate the bottom joints of the full-scale cage.

v. Cross-bracing

Cross-bracing was used on each side of the cage, running diagonally from the top of each spar to the bottom of the adjacent one. This helped maintain the shape and rigidity of the cage, and was present in the full-scale. Additional cross-bracing was deemed necessary in the model due to excessive motion in the joints. The cross-bracing ran from the top of each spar to the bottom of the opposing one, through the middle of the cage. It also ran from the bottom of one spar to the bottom of the opposing spar. All of this proved important to prevent the cage from slightly changing shape. It was determined that this excessive motion was due to the joints having too much play, as compared to the full-scale joints which allow for strictly vertical or strictly horizontal and vertical motion.

B. Netting

The netting that was used for the model was taken from the UNH pier. A large rectangle was trimmed to the height of the cage and was wide enough to wrap around all sides. An additional section was trimmed to fit the bottom of the cage. The seams of these large sections were then stitched together using a net mending needle. Using the screw eyes mounted on the inner sides of the spar caps, the net was tensioned using zip-ties all around the cage. This allowed for the net to be taught to the frame to prevent drifting or sagging when exposed to moving water. Once attached to the screw eyes, the net was tensioned over the pipe walkways using zip-ties, so it was even all around the cage, seen in Figure 6. A top net was not fabricated due to limited material and the need to access the interior of the cage.



Figure 6: Scale model with netting installed.

C. Mooring System

To fabricate the buoys, six 3x3x4 inch blocks of two-inch thick closed cell foam insulation board were glued together and then trimmed into a cylinder on the band saw. The cylinders were then sanded down on the belt sander to match the correct net buoyancy compared to the full scale, seen in Figure 7. The anchors for the mooring system were 25-30 lb lead blocks.



Figure 7: Buoys and bridle lines used in the scale model mooring system.

V. HYDROSTATIC TESTING

The StormSafe Submersible Net Pen relies on a compressor-powered airlift system to raise or submerge it via the simultaneous addition or removal of air in each spar. Ballast adjustment in the scale model was instead accomplished manually for time and cost purposes. Combinations of water and solid ballast in the form of steel nuts and bolts were used in order to establish the proper center of gravity of the model.

A. Surface

The full-scale StormSafe cage sits roughly 30 inch above the surface of the water in its surface configuration. This freeboard is accomplished by flooding the bottom third of the spars with water, adding approximately 3131 kg of ballast to each. The ballast of the model in the surface configuration was based upon maintaining a scaled down freeboard of 2 inches. A combination of 422 g of solid and 540 g of water ballast was used to accomplish this. Centers of gravity and buoyancy of the full scale, model scale, and actual model were calculated using Equations 1 and 2 and can be seen below in Table 4.

Equation 1: Center of Gravity

$$C_g = \frac{y_1 m_1 + y_2 m_2}{m_{total}}$$

y = center of component's mass

m = mass of component

m_{total} = total mass of model

Equation 2: Center of Buoyancy

$$C_b = \frac{c_1 SV_1 + c_2 SV_2}{V_{total}}$$

c = centroid of component

SV = submerged volume of component

V_{total} = total volume of model

	Full Scale	Model Scale	Actual
Total Ballast per Spar [kg]	3131.07	.928	.962
Cg [cm]*	642.62	42.85	42.8
Cb [cm]*	336.27	22.43	28.78

Table 4: Comparison between the centers of gravity and buoyancy of the full-scale, model scale, and actual model for the surface configuration.

*Center of gravity and center of buoyancy were both calculated without the net, and in reference to the bottom of the spars

B. Submerged

The full-scale submerged configuration depth modeled in this experiment was 15 ft below the surface. Accordingly, the model was submerged to a scaled depth of 1 ft below the surface. 780 g of water and 474 g of solid ballast put the model at this depth, with a difference in Cg of less than 3%. Centers of gravity of the full scale, model scale, and actual model can be seen below in Table 5.

	Full Scale	Model Scale	Actual
Total Ballast per Spar [kg]	4079.82	1.209	1.254
Cg [cm]*	607.75	40.51	41.61

Table 5: Comparison between the center of gravity of the full-scale, model scale, and actual model for the submerged configuration.

*Center of gravity was calculated without the net, and in reference to the bottom of the spars

VI. TANK TESTING

A. Currents

Exposing the model to fluid flow and examining the drag force it caused was important to the project due to the commonality of currents in net pen aquaculture. One of the tenants of this type of fish farming is the high exchange rate of water through the cage, so it is common practice to deploy net pens in high current environments. We were unable to expose the model to actual moving water; however, currents were simulated by towing the model through the UNH Wave Tank at certain Froude-scaled speeds. The maximum surface currents recorded at the Long Island site were 0.6 m/s. Velocity Froude-scales to the one half, so the model was towed at speeds of 5, 10, 15, and 20 cm/s, with 15cm/s corresponding to the maximum 0.6 m/s full-scale value. The model was towed through the tank three times at each speed for both its surface and submerged configurations. This resulted in a total of twelve current-simulating tow runs. The model was towed by the leading spar, with force being evenly distributed between the top and bottom of the spar via the tow bridle.

i. Methodology

In order to tow the model through the tank, a beam was affixed to the tow carriage and extended down into the water. A 7 ft piece of 80/20 aluminum served as the beam. The forces acting on the cage were recorded using a Futek 10 lb Submersible load cell, which was hooked up to the cDAQ system of the UNH Wave Tank to record data in LabView. The load cell was sized based on preliminary drag force calculations involving maximum velocities due to waves and currents as well as the maximum projected area of the model. A drag coefficient of 1.2, common for cylinders, was used for the prediction. The drag force equation can be seen below in Equation 3.

Equation 3: Drag Force

$$F_d = \frac{1}{2} C_d \rho A_p u^2$$

$C_d = \text{coefficient of drag}$

$\rho = \text{fluid density}$

$A_p = \text{projected area}$

$u = \text{fluid velocity}$

One end of the cell was mounted to the 80/20 beam, while the other end was attached to the tow bridle. The tow bridle was made using three pieces of the fishing monofilament, a small shackle, and two quick-disconnect fishing clips. This allowed the cage to be towed evenly through the water, distributing the force equally between the top and bottom of the leading spar. The quick-disconnect clips attached to the top and bottom screw eyes on the leading spar. Towing the model at the two desired depths was accomplished by raising or lowering the 80/20 beam to specific depths that corresponded to the center of the model during both configurations.

ii. Results

Ocean currents were simulated by towing the model through the UNH Wave Tank via the tow carriage. Towing at scale speeds of 5, 10, 15, and 20 cm/s, the following drag force results were acquired, seen in Figure 8.

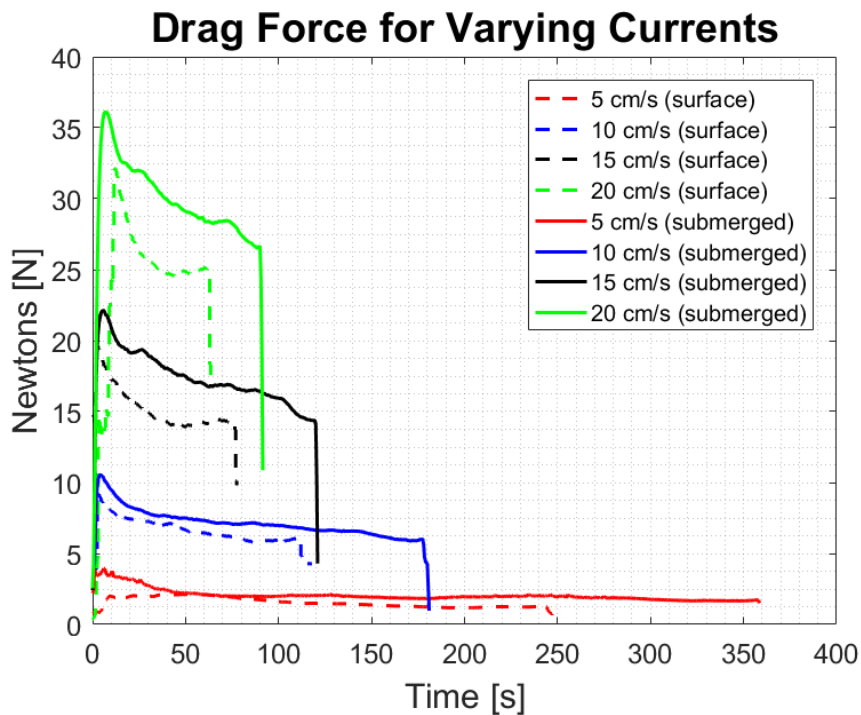


Figure 8: Drag force caused by the cage at varying tow speeds in both the surface and submerged configurations.

Figure 8 shows that as the speeds increase, the difference in drag force between the surface and submerged configurations became larger. This is due to the submerged case having a larger projected area. As a full-scale comparison, the steady state force at a current speed of 20 cm/s scales up to 94.5 kN (about 21,000 lbs) and a speed of 0.77 m/s. Whereas the force at the slower speed of 5 cm/s scales up to 7.7 kN (about 1700 lbs) and a speed of 0.2 m/s.

iii. Discussion

Therefore, the submerged configuration resulted in higher drag force due to the larger projected area encountered by the fluid. The forces also did not exceed the max tensile strength of the mooring lines, even when tested at speeds greater than those of the full-scale site. As a full-scale comparison, the 20 cm/s max tow speed corresponded to currents of 0.77 m/s full scale, which is greater than the max speed of 0.6 m/s recorded at the NY site.

B. Waves

i. Methodology

In order to properly examine the model's response to wave forcing, it had to be moored within the wave tank. This was done using a Froude-scaled version of the taut moored system that is utilized by the full-scale in the Great Lakes. The system relies on six deadweight anchors attached to an equal number of surface buoys. Bridle lines run 45 ft from the buoys to their respective spars, creating a bicycle spoke shape when viewed from above. The line diameter and net buoyancy of the taut moored system were Froude-scaled as well, in order to create a model scale mooring system. Length scales linearly in Froude scaling, therefore the bridle line lengths of the model scale mooring were 3 ft long, seen in Figure 9.

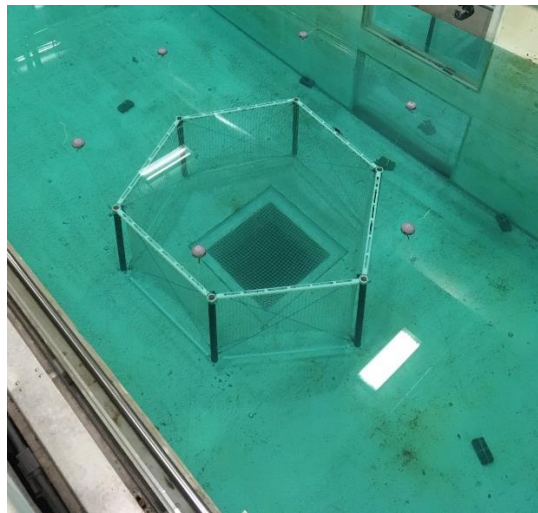


Figure 9: Birds-eye view of the scale model mooring system in a submerged configuration.

Wave induced loading in the mooring system was recorded with the same 10 lb submersible load cell used for tow testing. However, for wave testing the load cell was mounted to the top cap of the leading spar and the bridle line ran from the load cell to the leading buoy.

Once moored, the model was subjected to various wave heights and periods in order to simulate ocean conditions. The waves used were of 5, 10, and 15 cm heights at periods of 1.0 s to 2.5 s in quarter second intervals. The model saw these three waves heights and seven periods while moored in both the surface and submerged configurations, for a total of 42 normal wave runs. Four random wave runs, generated with the Bretschneider spectra, were conducted as well. Each

mooring configuration saw significant wave heights of 15 and 20 cm with peak periods of 1.5 s. The maximum wave height and period of 15 cm and 2.5 s was equivalent to a 2.25 m, 9.68 s wave. Model scale equivalent wave heights and periods can be seen below in Tables 6 and 7.

Scale and Run #	Type	Height [m]	Periods [s]
MS 1	Monochromatic	.05	1.0, 1.25, 1.5, 1.75, 2.0, 2.25, 2.5
FS 1	Monochromatic	.75	3.87, 4.84, 5.81, 6.78, 7.75, 8.71, 9.68
MS 2	Monochromatic	.1	1.0, 1.25, 1.5, 1.75, 2.0, 2.25, 2.5
FS 2	Monochromatic	1.5	3.87, 4.84, 5.81, 6.78, 7.75, 8.71, 9.68
MS 3	Monochromatic	.15	1.0, 1.25, 1.5, 1.75, 2.0, 2.25, 2.5
FS 3	Monochromatic	2.25	3.87, 4.84, 5.81, 6.78, 7.75, 8.71, 9.68

Table 6: Model scale and full-scale equivalent monochromatic wave testing conditions.

Scale and Run #	Type	Significant Wave Height [m]	Peak Period [s]
MS 4	Random (Bretschneider)	.15	1.5
FS 4	Random (Bretschneider)	2.25	5.81
MS 5	Random (Bretschneider)	.2	1.5
FS 5	Random (Bretschneider)	3.0	5.81

Table 7: Model scale and full-scale equivalent random wave testing conditions.

Mooring Forces

Using the waves specified above, in the mooring system described previously, the mooring loads were determined and are shown in Figure 10 below.

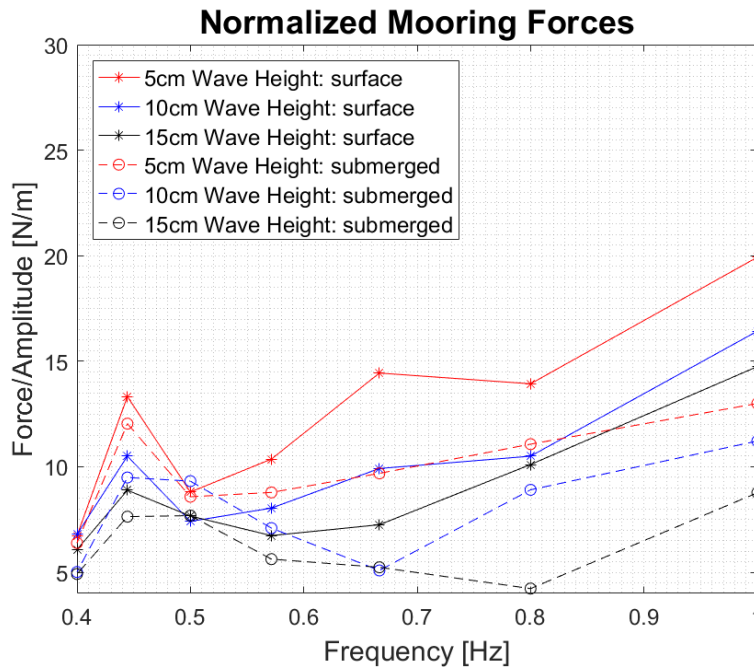


Figure 10: Normalized mooring forces as a function of frequency for both surface and submerged configurations.

Figure 10 shows that the dashed lines (submerged) remain below the solid lines (surface), more noticeably at frequencies of 0.8-1.0 Hz.

For the random wave testing, the loading for each configuration is shown below in Figures 11 and 12.

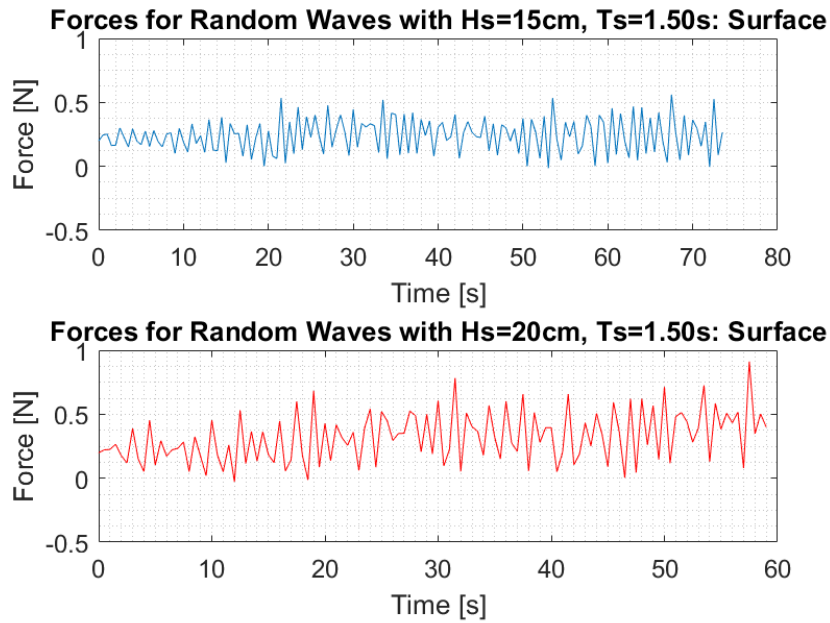


Figure 11: Time series of mooring forces for random waves in the surface configuration.

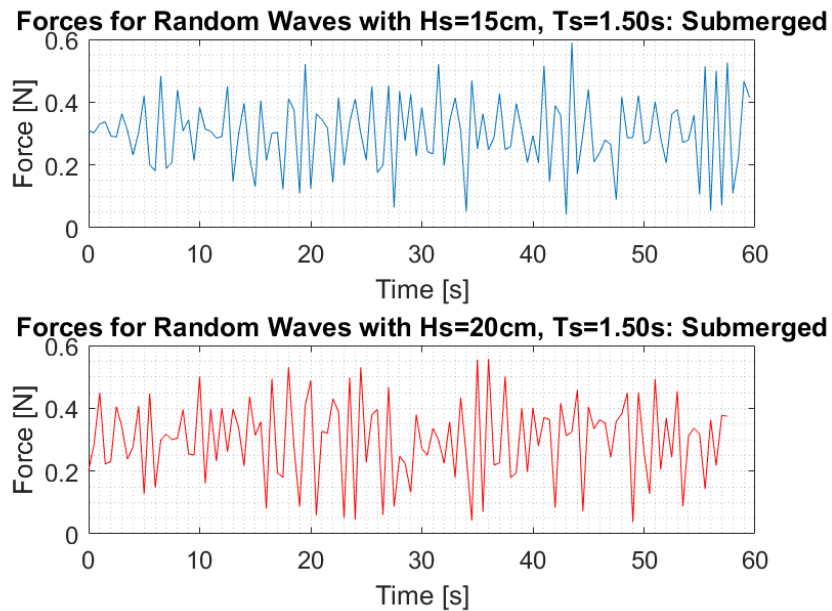


Figure 12: Time series of mooring forces for random waves in the submerged configuration.

Figures 11 and 12 show that the loading in the mooring system for both the surface and the submerged configurations are similar for the different random wave cases. However, due to the

fact that the wavemaker was not consistently outputting the correct wave height, it was noticed that there was an exaggeration in this error for random waves. Specifically, the paddle could not precisely output the desired significant wave heights and periods.

Motion Testing

The motion of the model was analyzed in order to determine its response to wave forcing. A 6x5 inch target with several black dots, seen in Figure 13, was attached to the middle of the pipe walkway nearest the viewing window of the wave tank. The target was mounted in the center of the pipe walkway in order to be in line with the center of gravity, thus ensuring accurate motion analysis.

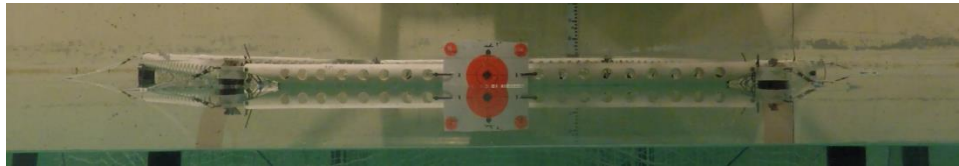


Figure 13: Target used for motion tracking.

A GoPro camera, set to record in linear mode, was mounted outside the window in order to capture the movement of the target for each of the different wave runs. The videos were then processed with a tracking program called Kinovea. The input of a known calibration distance and the selection of the point(s) of interest enabled the tracking of their positions throughout the video. Kinovea has an automated tracking function, however its effectiveness decreased greatly if the point of interest was obscured or even blurred at any time. Wave crests, refraction, and even the scum line on the viewing window caused the automatic tracking to fail, requiring manual tracking. A snapshot of the Kinovea tracking process can be seen below in Figure 14.

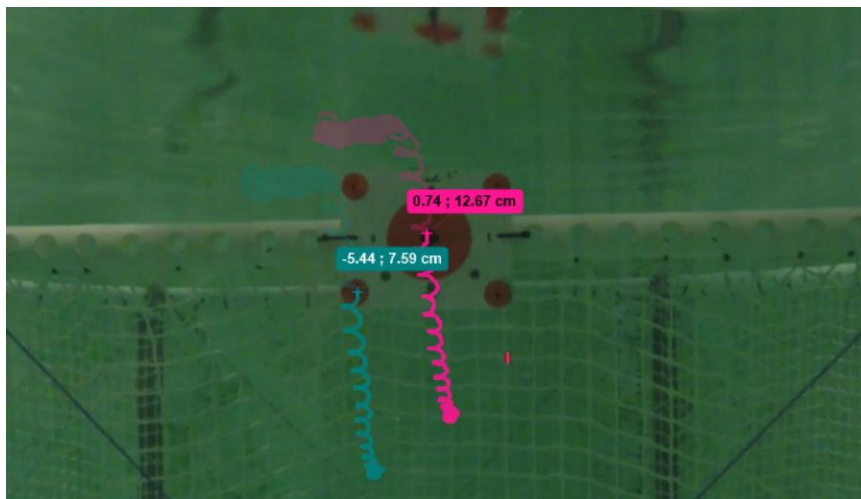


Figure 14: Kinovea position tracking paths for a 15 cm, 1.0 s wave in the submerged configuration.

The displacements of these points were analyzed to yield heave, surge, and pitch motion (with pitch defined as the rotation of the model in the leading and trailing spar plane). For heave and

surge only the center dot was tracked, resulting in x and y displacements (y for heave, x for surge). Pitch motion analysis required the positions of two points, so the center dot and either the top left or bottom left dots were tracked. The top left was the default second point for pitch tracking, with the bottom left used as an alternative whenever it was obscured less than the top. The varying geometry between the two points was interpreted to yield the change in angle of the model with respect to the vertical. The displacements of the model caused by these three motions were plotted as time series, an example of which can be seen below in Figure 15. The peaks and troughs of the motion signals were identified throughout a steady-state period in order to find their amplitudes.

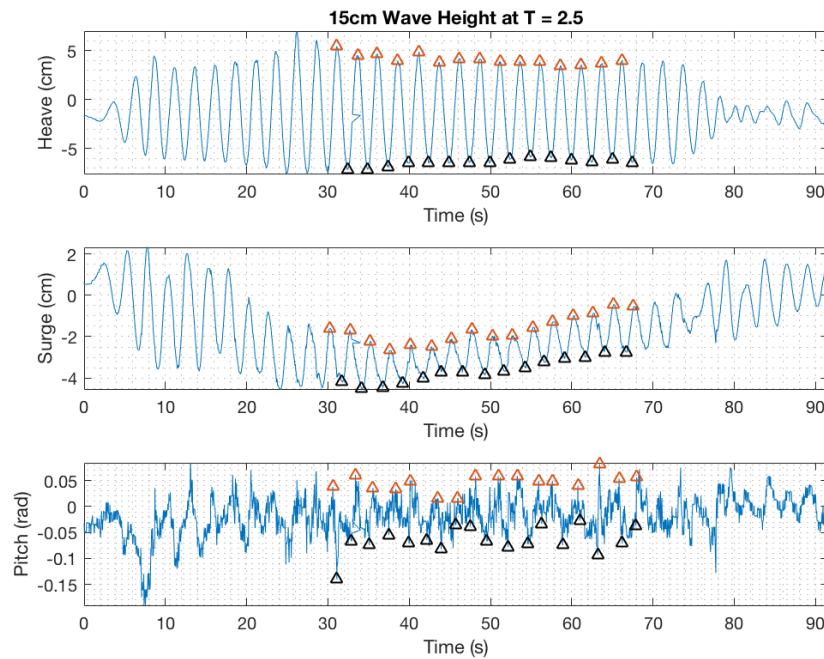


Figure 15: Time series of motion displacements for a 15 cm, 2.5 s wave in the surface configuration.

The amplitudes were then normalized by their respective wave forcing contributions to determine response amplitude operators or RAOs. The equations used to calculate heave, surge and pitch RAOs can be seen below in Equations 4, 5, and 6. Heave RAO was determined by normalizing the model’s vertical amplitude by the wave’s amplitude. Surge RAO was determined by normalizing the model’s horizontal amplitude by the horizontal motion of the fluid particles. Pitch RAO was determined by normalizing the model’s change in angle with respect to the vertical by the wave slope amplitude.

Equation 4: Heave RAO

$$\text{Heave RAO} = \frac{\text{Heave Amplitude}}{\text{Wave Amplitude}}$$

Equation 5: Surge RAO

$$\text{Surge RAO} = \frac{\text{Surge Amplitude}}{\zeta}$$

$$\zeta = \frac{H \cosh(kh + z)}{2 \sinh(kh)}$$

$$k = \frac{2\pi}{L}$$

Equation 6: Pitch RAO

$$\text{Pitch RAO} = \frac{\theta_{amp}}{ak}$$

$a = \text{wave amplitude}$

ii. Results

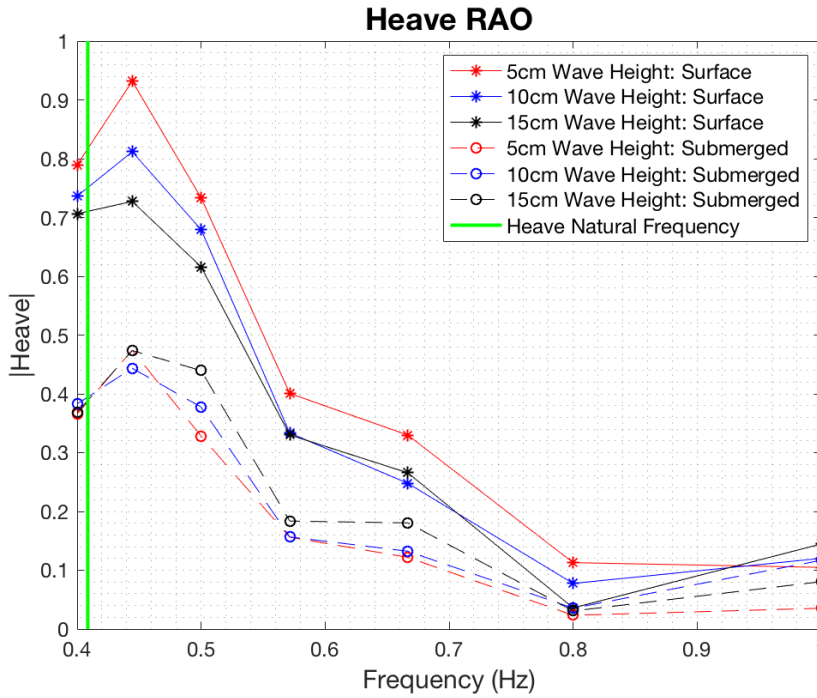


Figure 16: Heave RAO as a function of frequency for both the surface and submerged configurations.

The heave natural frequency of the model, represented by the green line on Figure 16, was calculated using Equations 7 and 8, and was found to occur at 0.41 Hz or 2.45 s.

Equation 7: Heave Natural Frequency

$$\omega_o = \sqrt{\frac{\rho g S}{m_{total}}}$$

$S = \text{model's waterplane area}$

Equation 8: Heave Natural Period

$$T_o = \frac{2\pi}{\omega_o}$$

For all the RAO plots, the solid lines indicate testing done with the model in the surface configuration, and the dashed lines indicate testing done in the submerged configuration. Figure 16 shows that submergence of the model resulted in decreased heave response.

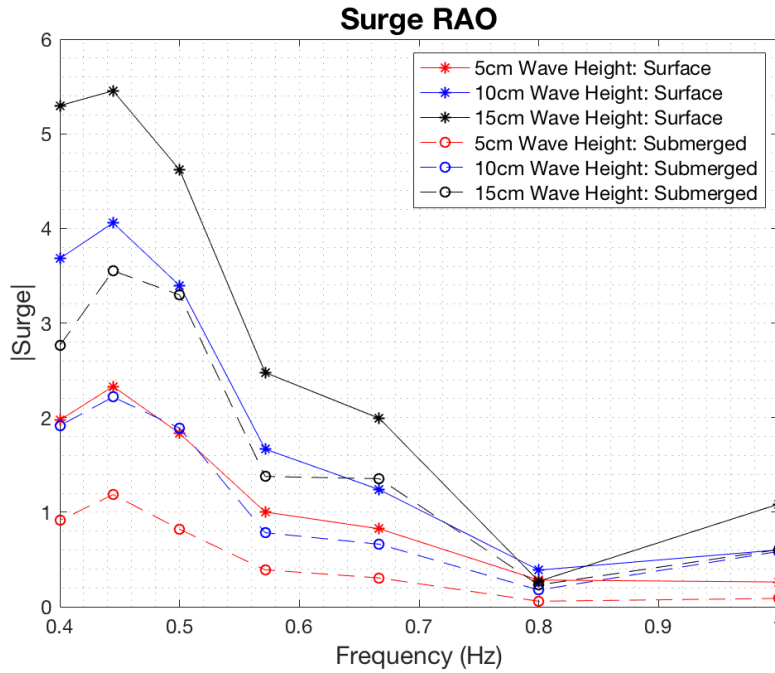


Figure 17: Surge RAO as a function of frequency for both the surface and submerged configurations.

Figure 17 shows that submergence of the model resulted in significantly decreased surge response, especially at lower frequencies.

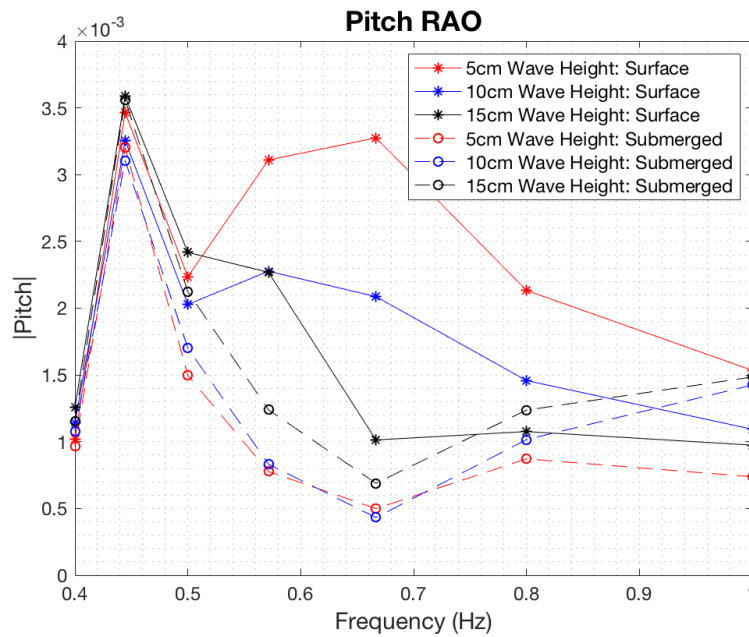


Figure 18: Pitch RAO as a function of frequency for both the surface and submerged configurations.

Figure 18 shows that submergence of the model generally resulted in decreased pitch response. However, pitch motions were orders of magnitude less than heave and surge motions and therefore resulted in less predictable behavior over the range of frequencies.

iii. Discussion

Figure 10 shows that the submerged case resulted in less loading in the mooring system, especially for high frequency waves. Even with the cage submerged a small depth relative to the size of the model (about 1 ft), the forces decrease significantly. This confirms that forces in the mooring decreases upon submergence of the cage.

For the random wave testing, since the wavemaker could not precisely output the desired significant wave heights and periods and we weren't able to recalibrate, it was determined that the results for random waves were inconclusive.

Heave motion throughout all the wave heights encountered should theoretically peak at the calculated heave natural frequency of the model. However, heave motion actually peaked at a higher frequency, 0.44 Hz instead of the calculated 0.41 Hz. This may be due to discrepancies in the output of the wave paddle compared to what was actually input.

Figures 16, 17, and 18 all exhibit lower motion values for testing done in the submerged configuration than testing done in the surface configuration. The decrease in wave induced motion of the model upon submergence is evident throughout all wave testing. Surge motion decreased as much as 45%, and heave motion decreased as much as 50%. Figure 19 provides a visual example of the minimal heave and surge motion seen in the submerged configuration during a low frequency wave. Negligible pitch motion was also observed throughout both wave testing configurations.

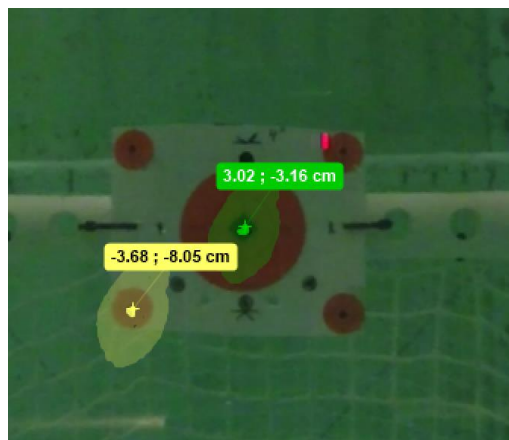


Figure 19: Motion observed for a low frequency wave in the submerged configuration.

VII. DISCUSSION

A. Hydrostatic Testing

Initial hydrostatic testing of the model for both its surface and submerged configurations made it clear that adjustments needed to be made. Both configurations were attempted with the proper Froude-scaled amount of water ballast in each spar. The result was excessive buoyancy and instability. To account for this, additional ballast was added in the form of water and steel nuts and bolts. The greater total ballast addressed the excess buoyancy and made the model sit at the proper levels, and the solid ballast served to lower the center of gravity and increase stability. The need for additional buoyancy stemmed from the fact that each pipe-based component had a greater diameter than what the model scale required, resulting in increased submerged volume and a greater overall buoyant force.

B. Current Testing

We did not have the ability to subject the model to actual flowing water, so currents were simulated by towing the model through the tank. In order to accomplish this the cage could not be moored to the bottom of the tank, and was therefore towed from the leading spar. Currents never act solely on one mooring line in the full scale, but testing in this configuration allowed for the determination of the maximum drag force that a mooring line might encounter.

C. Wave Testing

Throughout wave testing, it was observed that the wave paddle was producing smaller wave heights than what was being input. This discrepancy became even clearer for longer period waves, as differences of up to 4 cm between input and output wave height were noticed. Unfortunately, the wavemaker broke before we were able to confirm or recalibrate actual wave heights. This should be taken into account when considering all wave induced motion and loading results.

D. Discrepancies Between Model Scale Criteria and the Experimental Model

The construction of an experimental scale model of the StormSafe cage proved non-trivial. Aside from scaling down components, there were several issues unique to the scale model that had to be addressed.

The most significant of these issues was the assembly and transportation of the model. The full scale StormSafe is assembled in the water and never exists or is transported on land because of its sheer size. The model scale, being 1/15th the size, was certainly not going to be assembled in the water. It was constructed and assembled in UNH Ocean Structures Lab, and therefore needed to have the ability to be transported for testing in both the UNH Engineering and Wave Tanks. Assembly of the model scale was accomplished by adhering the six vertical spars to the floor in the proper hexagonal shape, and then connecting the horizontal pipe walkway and bottom connector pieces to the spars. In order to transport the model in a way that didn't apply uneven/excessive forces to the joints, a lift bridle was constructed. Even lengths of monofilament fishing leader were attached to the tops of each of the spars, and all came together at the center of

the cage. The lines were grouped together with a small shackle, as was a loop made of the same fishing leader. This allowed for the transport of the model by running a long pipe through the loop, and essentially lifting the model from above. This lift bridle design enabled successful transport and ensured that the weight of the cage was evenly distributed among all the joints when lifted. However, due to the need to consistently be able to move the cage, be it on land or into/out of the testing tanks, the lift bridle was a permanent fixture. As a result, there was some additional mass in the scale model that does not exist in the full scale.

Feasibility and time constraints of the project also affected some aspects of the scale model. The submersible capability of the full scale StormSafe cage relies on the addition or removal of air from within the spars. This simultaneous adjustment of air occurs with the use of a small air compressor attached to a manifold that connects an air hose to each of the six spars. Adding air to the spars decreases the amount of water ballast, thus raising the cage, while letting air out allows water to fill the spars and submerges the cage. The fabrication of a model scale airlift system was impractical and would have required time that was needed for testing. Therefore, ballast was manually added and removed from the scale model.

The selection of materials proved to be quite challenging. Satisfying key parameters of the full-scale cage while adhering to financial, time, and logistical constraints led to some flaws in the fabrication of the scale model. The net used in the model was likely the most significant of these flaws. In order to conserve time and money, the netting was sourced from a stock of previously used net at the UNH Coastal Marine Lab. The net selected was the most suitable candidate of those available, however the spacing between the threads was greater than that of the full scale. The net used had a slightly larger thread diameter which helped to compensate for the difference in solidity ratio between the full and model scale, however the effects of larger thread spacing prevailed. The result was a scale model projected area that was roughly 15% lower than what the Froude scaling dictated. The use of PVC for the pipe walkway and bottom connector components was also a source of error. Since the mass of the pipe walkway components had to account for the mass of the decking in the full scale, a relatively dense material was needed. PVC was used because it was the most readily available material that satisfied this requirement, but it was still too dense. The effect of this elevated density was compounded by the fact that all plastic pipe is manufactured to conventional sizes. Acquiring pipe that was the exact density and diameter specified by the Froude scaling was not feasible, so the error of conventional pipe size affected all of the pipe-based components to some degree. The mass of the spars, pipe walkways, and bottom connectors, were all greater than the Froude-scale specification, resulting in a total weight (not including the net) that was roughly 8% too high. Additionally, the bottom connectors had a greater-than-scale diameter which caused a projected area that was roughly 22% too large. While this is certainly not ideal, it likely mitigated the effects of the lower net projected area to some extent.

Lastly, a full scale StormSafe cage moored out in the open ocean would almost never encounter just current or just waves. Realistically it would always be experiencing the effects of both simultaneously. We had hoped to perform simultaneous wave and current testing by towing the model through the tank while making waves. However, the wavemaker broke before we were able to obtain enough data. The model's response to storm waves is another crucial component

that should have been examined in order to aid in the ocean-ready evaluation. The UNH Wave Tank is not capable of simulating storm waves even when in fully-operating condition though.

VIII. CONCLUSION

Scale model testing of the StormSafe Submersible Net Pen shows promise for its use in an open ocean environment 8 miles off the coast of Long Island, NY. The model fabricated and tested in this project was not an exact 1/15th Froude-scaled model and storm waves were not simulated, so no definitive conclusions can be drawn about its adequacy for an ocean environment. However, Sea State 4 equivalent wave and high current testing did provide promising proof-of-concept for the use of StormSafe in the ocean. Forces within the mooring system never experienced loads greater than the maximum tensile strength of the mooring lines, even when exposed to currents greater than those previously recorded at the intended site. Wave induced motion and loading decreased significantly upon submerging the cage only an eighth of the total depth, proving that the submersible capability can effectively remove it from high energy environments. These results indicate that StormSafe Submersible has serious potential for offshore net pen aquaculture.

A. Global Impact

The successful implementation of the StormSafe Submersible Net Pen in open ocean environments could revolutionize the aquaculture industry. While there are other submersible net pen designs, StormSafe stands out in several ways. Its stability, modularity, and submersible capabilities make it a viable option for the growout of saltwater finfish almost anywhere in the world. With a capacity of nearly one million pounds of fish, the StormSafe cage could truly help to address the world's growing food crisis.

IX. REFERENCES

- Heller, V. Model-Prototype Similarity. 2012. http://drvalentinheller.com/Dr%20Valentin%20Heller_files/Heller_Model-Prototype%20Similarity.pdf
- Meeker, M. Fully Submersible Net Pen. 2019, <https://www.stormsafesubmersibles.com>
- NTNU. General Modelling and Scaling Laws. 2019, https://www.ivt.ntnu.no/imt/courses/tmr7/lecture/Scaling_Laws.pdf
- Polyform. Aqua-Series. 2019, <https://polyform.no/hard-shell-pe-products/aqua-series/>